

Structural Trends in $\text{TeI}_2\text{RR}'$: Crystal Structures and NMR Spectra of $\text{TeI}_2(\text{CH}_2\text{SiMe}_3)_2$, $\text{TeI}_2\text{Th}(\text{CH}_2\text{SiMe}_3)$, $\text{TeI}_2\text{Ph}(\text{CH}_2\text{SiMe}_3)$, and TeI_2Th_2 (Th = 2-Thienyl, $\text{C}_4\text{H}_3\text{S}$)

Merja J. Poropudas, Ludmila Vigo, Raija Oilunkaniemi, and Risto S. Laitinen

Department of Chemistry, P.O. Box 3000, FI-90014 University of Oulu, Oulu, Finland

Received 29 September 2010; revised 7 November 2010

ABSTRACT: $\text{TeI}_2(\text{CH}_2\text{SiMe}_3)_2$ (**1**), $\text{TeI}_2\text{Th}(\text{CH}_2\text{SiMe}_3)$ (**2**), $\text{TeI}_2\text{Ph}(\text{CH}_2\text{SiMe}_3)$ (**3**), and TeI_2Th_2 (**4**) (Th = 2-thienyl) were synthesized in excellent yields from the corresponding tellanes and I_2 . The products were characterized by ^{125}Te NMR spectroscopy and single crystal X-ray crystallography. Each $\text{TeI}_2\text{RR}'$ molecule shows a trigonal bipyramidal coordination around tellurium with the iodine atoms occupying axial positions, and the organic groups and the lone pair occupying equatorial positions. The Te–I bonds and the I–Te–I angles in **1–4** span a range of 2.8407(9)–3.0194(10) Å and 171.85(2)–175.71(2)°, respectively. The Te–C bonds and C–Te–C angles show respective ranges of 2.100(6)–2.136(7) Å and 95.1(3)–100.9(3)°. In the solid state, the molecules show a varying degree of secondary bonding interactions. With the exception of $\text{TeI}_2(\text{CH}_2\text{SiMe}_3)_2$ (**1**), the compounds show $\text{Te}\cdots\text{I}$ or $\text{I}\cdots\text{I}$ secondary bonding interactions leading to supramolecular assemblies. $\text{TeI}_2\text{Ph}(\text{CH}_2\text{SiMe}_3)$ crystallizes as two polymorphs. One (**3a**) is isomorphic

with $\text{TeI}_2\text{Th}(\text{CH}_2\text{SiMe}_3)$ (**2**). The other (**3b**) shows a lattice of two alternating layers of molecules. In one layer, the molecules are linked into a two-dimensional network by $\text{Te}\cdots\text{I}$ and $\text{I}\cdots\text{I}$ interactions whereas the second layer consists of discrete dimers. The strongest $\text{Te}\cdots\text{I}$ secondary bonding interactions are observed for TeI_2Th_2 . The lattice is composed of tetramers that is reminiscent of those in γ - and δ - TeI_4 and also have precedent in $\text{TeI}_2\text{RR}'$ species. The structures of TeI_2Me_2 and TeI_2Ph_2 have been considered for comparison. The trends in ^{125}Te NMR chemical shifts in $\text{TeI}_2\text{RR}'$ (R, R' = Me, CH_2SiMe_3 , Th, Ph) are also discussed. © 2011 Wiley Periodicals, Inc. Heteroatom Chem 22:348–357, 2011; View this article online at wileyonlinelibrary.com. DOI 10.1002/hc.20688

Dedicated to Professor Kin-ya Akiba on the occasion of his 75th birthday.

Correspondence to: R. Oilunkaniemi; e-mail: raija.oilunkaniemi@oulu.fi, Risto S. Laitinen; e-mail: risto.laitinen@oulu.fi.

Contract grant sponsor: Academy of Finland.

Contract grant sponsor: Ministry of Education.

© 2011 Wiley Periodicals, Inc.

INTRODUCTION

Diorganytellanes react with iodine to afford diiododiorganytellurium(IV), $\text{TeI}_2\text{RR}'$ [1,2]. In these molecules, the primary bonding environment of tellurium is a distorted trigonal bipyramid in which the organic groups and the lone-pair of tellurium occupy the equatorial positions whereas the iodine atoms lie at the axial positions (for selected molecular species (see [3–14]). In the solid state, TeI_2R_2 molecules generally show intermolecular $\text{Te}\cdots\text{I}$ or $\text{I}\cdots\text{I}$ secondary bonding interactions (the concept of which

was originally introduced by Alcock [15]) that generally expand the AX_4E (X = bonding pair, E = lone pair) trigonal pyramidal geometry around tellurium into five- or six-coordinate AX_4YE or $\text{AX}_4\text{Y}_2\text{E}$ (X = primary bond, Y = secondary bond) environments and lead to the formation of supramolecular frameworks [3]. These frameworks can typically be chains, layers, or three-dimensional networks. Depending on the nature of the organic groups, other intermolecular interactions can contribute to the formation of supramolecular assemblies [16].

In the present work, we have explored effect of the nature of the organic groups on solid-state structures of $\text{TeI}_2\text{RR}'$. We report the preparation of $\text{TeI}_2(\text{CH}_2\text{SiMe}_3)_2$ (**1**), $\text{TeI}_2\text{Th}(\text{CH}_2\text{SiMe}_3)$ (**2**), $\text{TeI}_2\text{Ph}(\text{CH}_2\text{SiMe}_3)$ (**3**), and TeI_2Th_2 (**4**) (Th = 2-thienyl, $\text{C}_4\text{H}_3\text{S}$) by the reaction of corresponding diorganyltellanes with I_2 . The products were characterized by ^{125}Te NMR spectroscopy and single crystal X-ray crystallography. For comparison, the structures and ^{125}Te NMR spectroscopic properties of TeI_2Me_2 , TeI_2PhMe , and TeI_2Ph_2 are also discussed as appropriate.

EXPERIMENTAL

General

All reactions were carried out under an argon atmosphere. Diethylether (Lab-Scan, Gliwice, Poland), *n*-hexane (Lab-Scan), dichloromethane (Lab-Scan), and iodine (Aldrich, Schnelldorf, Germany) were commercially available and were used without further purification. Tetrahydrofuran (Lab-Scan) was dried and distilled over Na/benzophenone under an argon atmosphere prior to use. $\text{Te}(\text{CH}_2\text{SiMe}_3)_2$ was prepared according to the literature method [17]. TeTh_2 was prepared from Te_2Th_2 [18] by copper(0)-promoted detelluration [19]. $\text{TeTh}(\text{CH}_2\text{SiMe}_3)$ and $\text{TePh}(\text{CH}_2\text{SiMe}_3)$ were prepared from bis(2-dithienyl) ditellane and diphenyl ditellane, respectively, by using the method described by Ogura et al. [20]. The NMR spectroscopic data of the tellanes (CDCl_3 , 25°C , ppm): $\text{Te}(\text{CH}_2\text{SiMe}_3)_2$: δ $^{13}\text{C}\{^1\text{H}\}$ 15.8 (CH_2), -3.5 (SiMe_3); ^{125}Te 26. $\text{TeTh}(\text{CH}_2\text{SiMe}_3)$: δ $^{13}\text{C}\{^1\text{H}\}$ 140.6, 133.8, 128.8, 98.7 ($\text{C}_4\text{H}_3\text{S}$), -0.4 (SiMe_3), -5.1 (CH_2); ^{125}Te 234. $\text{TePh}(\text{CH}_2\text{SiMe}_3)$: δ $^{13}\text{C}\{^1\text{H}\}$: 137.0, 129.2, 127.3, 113.2 (C_6H_5), -0.3 (SiMe_3), -8.8 (CH_2); ^{125}Te 344. TeTh_2 : δ $^{13}\text{C}\{^1\text{H}\}$: 140.9, 134.6, 129.0 103.0 (C_6H_5); ^{125}Te 408.

NMR Spectroscopy

^{125}Te NMR spectra were recorded on a Bruker DPX400 spectrometer operating at 126.28 MHz. The

^{13}C and ^{125}Te spectral widths were 24.04 and 126.58 kHz, respectively, the pulse widths 10.00 μs , and the pulse delays were 1.60 s. In both cases, ^{13}C accumulations typically contained ca. 1,000 transients and ^{125}Te accumulations ca. 30,000 transients. All spectra were recorded unlocked. A saturated solution of diphenylditellane in CDCl_3 was used as an external standard for ^{125}Te . Chemical shifts (ppm) are reported relative to neat Me_2Te [δ (Me_2Te) = δ (Ph_2Te_2) + 422] [21].

X-Ray Crystallography

Diffraction data of **1–4** were collected at 120 K on a Bruker Nonius Kappa-CCD diffractometer using graphite monochromated Mo K_α radiation ($\lambda = 0.71073$ Å; 55 kV, 25 mA). Crystallographic data and details of crystal structure determinations are given in Table 1. The structures were solved by direct methods using SIR-92 [22], and refined using SHELXL-97 [23]. After the full-matrix least-squares refinement of the non-hydrogen atoms with anisotropic thermal parameters, the hydrogen atoms were placed in calculated positions in the aromatic rings ($\text{C–H} = 0.95$ Å), in CH_3 groups ($\text{C–H} = 0.98$ Å), and in CH_2 groups ($\text{C–H} = 0.99$ Å). In the final refinement, the calculated hydrogen atoms were riding with the carbon atom they were bonded to. The isotropic thermal parameters of the hydrogen atoms were fixed at 1.2 times to that of the corresponding carbon atom in the aromatic rings and to 1.5 times to that in methyl or methylene groups. The scattering factors for the neutral atoms were those incorporated with the programs.

The thienyl rings $\text{C}_4\text{H}_3\text{S}$ in **4** were found to be disordered. The disorder was refined by constraining the sum of the site occupation factors of each disordered pair to unity. Since the site occupation factors and thermal parameters of the disordered atoms correlate with each other, the thermal parameters of the corresponding pairs of atoms were restrained to be equal. The positional parameters of the disordered pairs of atoms were also constrained to be equal.

Crystallographic information of **1–4** has been deposited with the Cambridge Crystallographic Data Center as supplementary publication numbers CCDC 794943–794947. Copies of the data can be obtained free of charge on application to CCDC, 12 Union Road, Cambridge CB2 1EZ, UK [Fax: int. code + 44(1223)336-033; e-mail: deposit@ccdc.cam.ac.uk].

Preparation of $\text{TeI}_2(\text{CH}_2\text{SiMe}_3)_2$ (**1**)

Bis(trimethylsilylmethyl)tellane (0.094 g; 0.311 mmol) was dissolved in 3 mL of THF, and the

TABLE 1 Details of the Structure Determination of $\text{TeI}_2(\text{CH}_2\text{SiMe}_3)_2$ (**1**), $\text{TeI}_2\text{Th}(\text{CH}_2\text{SiMe}_3)$ (**2**), $\text{TeI}_2\text{Ph}(\text{CH}_2\text{SiMe}_3)$ (**3a** and **3b**), and TeI_2Th_2 (**4**) (Th = thienyl, $\text{C}_4\text{H}_3\text{S}$)

	1	2	3a	3b	4
Empirical formula	$\text{C}_8\text{H}_{22}\text{I}_2\text{Si}_2\text{Te}$	$\text{C}_8\text{H}_{14}\text{I}_2\text{SSiTe}$	$\text{C}_{10}\text{H}_{16}\text{I}_2\text{SiTe}$	$\text{C}_{10}\text{H}_{16}\text{I}_2\text{SiTe}$	$\text{C}_8\text{H}_6\text{S}_2\text{I}_2\text{Te}$
Formula weight	555.84	551.74	545.72	545.72	547.65
Crystal system	Triclinic	Triclinic	Triclinic	Monoclinic	Triclinic
Space group	$P\bar{1}$	$P\bar{1}$	$P\bar{1}$	$C2/c$	$P\bar{1}$
<i>a</i> (Å)	7.2326(14)	7.9645(16)	8.0401(16)	38.914(8)	9.4543(19)
<i>b</i> (Å)	9.870(2)	9.6148(19)	9.6010(19)	6.9889(14)	11.688(2)
<i>c</i> (Å)	12.813(3)	10.651(2)	10.862(2)	24.514(5)	12.698(3)
α (°)	106.96(3)	78.66(3)	79.09(3)		86.44(3)
β (°)	94.41(3)	68.34(3)	69.11(3)	108.46(3)	68.61(3)
γ (°)	92.25(3)	86.59(3)	85.54(3)		74.89(3)
<i>V</i> (Å ³)	870.5(3)	743.2(3)	769.2(3)	6324(2)	1260.5(4)
<i>Z</i>	2	2	2	16	4
<i>F</i> (000)	512	500	496	3968	976
<i>D</i> _{calc.} (g cm ⁻³)	2.121	2.466	2.356	2.293	2.886
μ (Mo <i>K</i> α) (mm ⁻¹)	5.364	6.341	5.995	5.833	7.546
Crystal size (mm)	0.50 × 0.50 × 0.10	0.10 × 0.10 × 0.09	0.20 × 0.20 × 0.15	0.20 × 0.10 × 0.05	0.20 × 0.10 × 0.08
Θ range (°)	1.67–26.00	3.28–25.99	2.04–25.99	3.04–26.00	3.35–25.99
Reflections collected	13573	12372	10852	23110	18586
Unique reflections	3376	2892	2972	6209	4894
Observed reflections	2745	2444	2553	4669	4267
Parameters/restraints	124/0	122/0	130/0	259/0	240/40
Goodness-of-fit on <i>F</i> ²	1.093	1.031	1.124	1.031	1.093
<i>R</i> _{int}	0.0694	0.0665	0.0969	0.0803	0.0841
<i>R</i> ₁ ^{a,b}	0.0546	0.0387	0.0623	0.0418	0.0503
<i>wR</i> ₂ ^{a,b}	0.1366	0.0994	0.1753	0.0934	0.1287
<i>R</i> ₁ (all data) ^b	0.0680	0.0492	0.0733	0.0674	0.0577
<i>wR</i> ₂ (all data) ^b	0.1577	0.1067	0.1927	0.1060	0.1349

^a $I \geq 2\sigma(I)$.

^b $R_1 = \sum ||F_o| - |F_c|| / \sum |F_o|$, $wR_2 = [\sum w(F_o^2 - F_c^2)^2] / \sum wF_o^2$.

resulting solution was added dropwise into a solution of iodine (0.080 g; 0.315 mmol) in 3 mL of THF. The reaction mixture was stirred for 2 h at room temperature and then sequentially concentrated by evaporation of the solvent. The reaction product was precipitated by adding a few drops of cold *n*-hexane to the cooled concentrated solution. The crude product was filtered, washed with cold *n*-hexane, and recrystallized from diethyl ether, giving orange crystals of **1** (yield 91%, 0.157 g). Anal. Calcd. for $\text{TeI}_2\text{Si}_2\text{C}_8\text{H}_{22}$; C 17.29, H 3.99; found C 17.25, H 3.99. NMR (CDCl_3 , 25°C, ppm): $\delta^{13}\text{C}\{^1\text{H}\}$ 26.2 (CH_2), 1.3 (SiMe_3); ^{125}Te 655.

The following reactions were performed in a similar fashion.

Preparation of $\text{TeI}_2\text{Th}(\text{CH}_2\text{SiMe}_3)$ (**2**)

Thienyl(trimethylsilylmethyl)tellane (0.097 g; 0.326 mmol), I_2 (0.085 g; 0.335 mmol). Dark orange crystals of **2** were obtained from CH_2Cl_2 (yield 90%,

0.161 g). Anal. Calcd. for $\text{TeI}_2\text{SiSC}_8\text{H}_{14}$; C 17.42, H 2.56; found C 17.69, H 2.60. NMR (CDCl_3 , 25°C, ppm): $\delta^{13}\text{C}\{^1\text{H}\}$: 140.4, 134.8, 128.1, 109.2 (C_6H_5), 32.9 (CH_2), -0.8 (SiMe_3); ^{125}Te 729.

Preparation of $\text{TeI}_2\text{Ph}(\text{CH}_2\text{SiMe}_3)$ (**3**)

Phenyl(trimethylsilylmethyl)tellane (0.095 g; 0.325 mmol), I_2 (0.081 g; 0.319 mmol). Recrystallization from CH_2Cl_2 yielded dark red crystals of **3a** and orange crystals of **3b** (combined yield 99%, 0.173 g). Anal. Calcd. for $\text{TeI}_2\text{SiC}_{10}\text{H}_{16}$; C 22.01, H 2.96; found C 22.75, H 3.04. NMR (CDCl_3 , 25°C, ppm): $\delta^{13}\text{C}\{^1\text{H}\}$: 134.4, 131.6, 130.6, 124.9 (C_6H_5), 28.4 (CH_2), 1.7 (SiMe_3); ^{125}Te 690.

Preparation of TeI_2Th_2 (**4**)

Bis(2-thienyl)tellane (0.098 g; 0.335 mmol), I_2 (0.091 g; 0.358 mmol). Recrystallization from THF yielded

dark red crystals of **4** (yield 94%, 0.173 g). Anal. Calcd. for $\text{TeI}_2\text{S}_2\text{C}_8\text{H}_6$; C 17.54, H 1.10; found C 17.96, H 1.14. NMR (CDCl_3 , 25°C , ppm): $\delta^{13}\text{C}\{\text{H}\}$: 141.2, 135.2, 128.1, 118.2 ($\text{C}_4\text{H}_3\text{S}$); ^{125}Te 892.

RESULTS AND DISCUSSION

General

The reactions of diorganyl tellanes $\text{Te}(\text{CH}_2\text{SiMe}_3)_2$, $\text{TeTh}(\text{CH}_2\text{SiMe}_3)$, $\text{TePh}(\text{CH}_2\text{SiMe}_3)$, and TeTh_2 with iodine afford the corresponding diiodidoorganyl-tellurium(IV) **1–4** in excellent yields. The products are relatively stable in air at room temperature. The choice of the solvent for recrystallization to obtain pure crystalline products was dependent on the organic group. Diiodidobis(trimethylsilylmethyl) tellurium(IV) (**1**) was recrystallized from diethylether, diiodidothienyl(trimethylsilylmethyl) tellurium(IV) (**2**), diiodidophenyl(trimethylsilylmethyl)-tellurium(IV) (**3**) from dichloromethane, and diiodidobis(2-thienyl)tellurium(IV) (**4**) was recrystallized from tetrahydrofuran. Upon recrystallization of **3**, two crops of crystals were obtained: dark red crystals **3a** and orange crystals **3b**.

Crystal Structures

The molecular structures of **1–4** indicating the numbering of the atoms and selected bond distances and angles are shown in Figs. 1–3.

The coordination environment around the tellurium in each compound is expectedly a pseudotrigonal bipyramid with the tellurium lone-pair and the two bonding pairs involving organic groups occupying equatorial positions. Iodine atoms are found in the axial positions. The stereochemical activity of the lone pair of the tellurium atoms results in the axial iodine atoms to lean away from the lone pair reducing the I–Te–I bond angles from the ideal value of 180° . The C–Te–C bond angles are also smaller than the ideal 120° .

The axial Te–I bond lengths [2.8904(10) and 2.9487(10) Å in **1**, 2.9098(8) and 2.9512(8) Å in **2**, 2.9266(9) and 2.9288(10) Å in **3a**, 2.8992(8)–2.9309(8) Å in **3b**, and 2.8407(9)–3.0194(10) Å in **4**] are expectedly longer than single bonds (the sum of the covalent radii of tellurium and iodine is 2.70 Å [24]). It has previously been reported that the I–Te–I moiety is often asymmetric, the shorter bonds ranging 2.85–2.90 Å and the longer bonds 2.91–3.01 Å [25,26]. The variation in the Te–I bond lengths are normally correlated with the I···Te and I···I secondary bonding, but hydrogen bonds and other possible secondary bonding interactions also have a

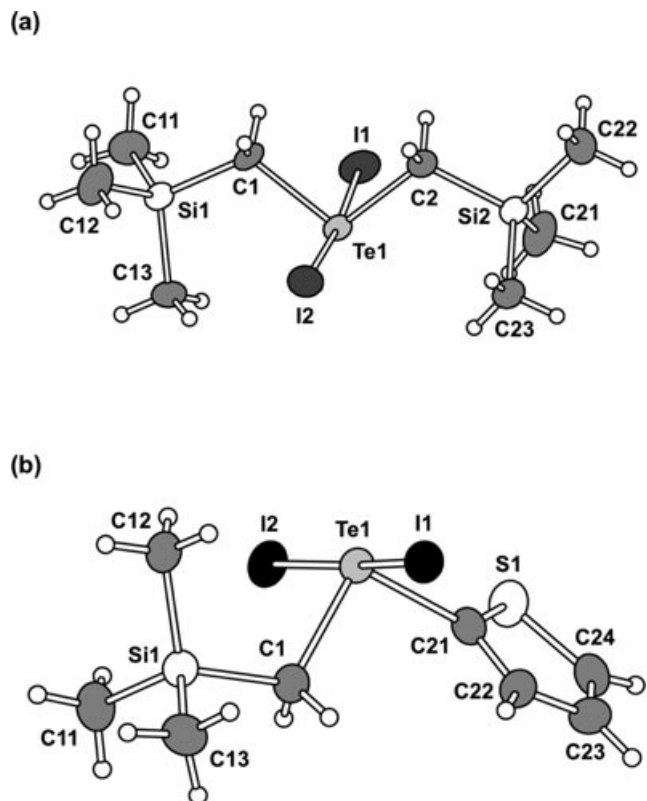


FIGURE 1 (a) The molecular structure of $\text{Te}_2(\text{CH}_2\text{SiMe}_3)_2$ (**1**) indicating the numbering of atoms. The thermal ellipsoids have been drawn at 50% probability level. Selected bond distances (Å) and angles ($^\circ$): Te1–I1 2.8904(10), Te1–I2 2.9487(10) Te1–C1 2.129(6), Te1–C2 2.132(7), I1–Te1–I2 175.34(2), I1–Te1–C1 88.3(2), I1–Te1–C2 91.0(2), I2–Te1–C1 86.9(2), I2–Te1–C2 89.5(2), C1–Te1–C2 99.9(3). (b) The molecular structure of $\text{Te}_2\text{Th}(\text{CH}_2\text{SiMe}_3)$ (**2**) indicating the numbering of atoms. The thermal ellipsoids have been drawn at the 50% probability level. Selected bond distances (Å) and angles ($^\circ$): Te1–I1 2.9512(8), Te1–I2 2.9098(8) Te1–C1 2.136(7), Te1–C21 2.100(6), I1–Te1–I2 172.24(2), I1–Te1–C1 87.6(2), I1–Te1–C21 94.2(2), I2–Te1–C1 89.7(2), I2–Te1–C21 93.3(2), C1–Te1–C21 95.3(2).

strong influence on the bond lengths and the formation of supramolecular assemblies [3–14].

The Te···I and I···I secondary bonding interactions in **1–4**, TeI_2Me_2 [14, 25], and TeI_2Ph_2 [26] are summarized in Table 2. It can be seen that Te···I close contacts are more common than I···I close contacts. This seems to be a general feature in all $\text{Te}_2\text{RR}'$ [3–14]. McCullough et al. [27] have correlated the presence of I···I secondary bonds with the color of the crystalline material. In the absence of I···I close contacts, the crystals appear orange or bright red. With increasing influence of the I···I interactions, the color becomes deeper red and tends toward purple and black. The colors of the present compounds are

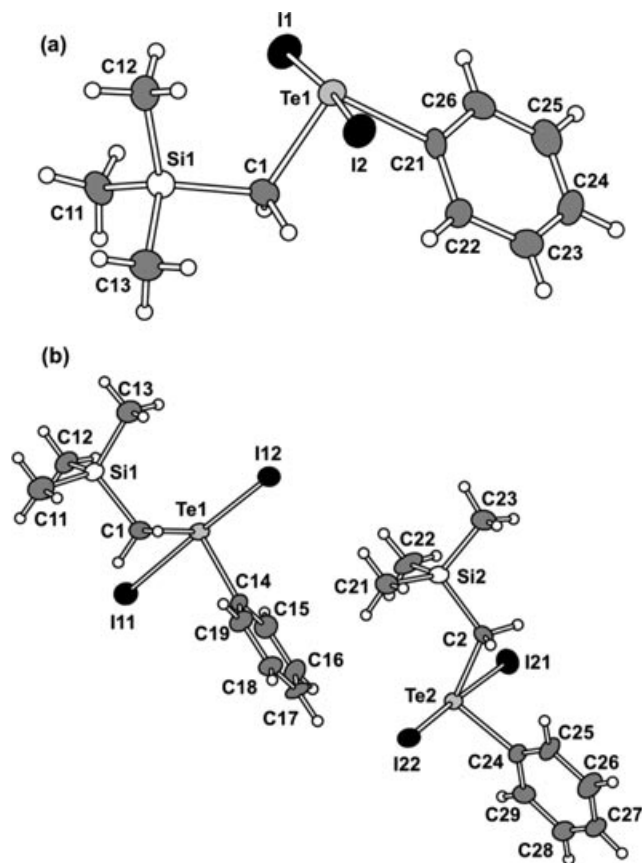


FIGURE 2 (a) The molecular structure of $\text{Te}_2\text{Ph}(\text{CH}_2\text{SiMe}_3)$ (**3a**) indicating the numbering of atoms. The thermal ellipsoids have been drawn at the 50% probability level. Selected bond distances (Å) and angles ($^\circ$): Te1–I1 2.9288(10), Te1–I2 2.9266(9), Te1–C1 2.135(8), Te1–C21 2.126(8), I1–Te1–I2 172.69(3), I1–Te1–C1 88.8(2), I1–Te1–C21 93.3(2), I2–Te1–C1 88.3(2), I2–Te1–C21 93.7(2), C1–Te1–C21 96.1(3). (b) The molecular structure of $\text{Te}_2\text{Ph}(\text{CH}_2\text{SiMe}_3)$ (**3b**) indicating the numbering of atoms. The thermal ellipsoids have been drawn at the 50% probability level. Selected bond distances (Å) and angles ($^\circ$): Te1–I11 2.9309(8), Te1–I12 2.8992(8), Te2–I21 2.9020(8), Te2–I22 2.9293(8), Te1–C1 2.135(7), Te1–C14 2.127(6), Te2–C2 2.124(6), Te2–C24 2.119(7), I11–Te1–I12 174.40(2), I11–Te1–C1 87.4(2), I11–Te1–C14 88.0(2), I12–Te1–C1 88.5(2), I12–Te1–C14 89.0(2), C1–Te1–C14 100.9(3), I21–Te2–I22 174.01(2), I21–Te2–C2 87.1(2), I21–Te2–C24 88.6(2), I22–Te2–C2 88.3(2), I22–Te2–C24 88.3(2), C2–Te2–C24 99.4(3).

mainly consistent with this scheme; we note that **4** is deep red, although there are no I...I secondary bonding interactions in the lattice.

$\text{Te}_2(\text{CH}_2\text{SiMe}_3)_2$ (**1**) shows hardly any secondary bonding interactions (see Table 2). The shortest respective Te...I and I...I intermolecular contacts in **1** are only slightly shorter than the sum of the van der Waals radii of the relevant atoms but significantly longer than those of **2–4** and the values reported

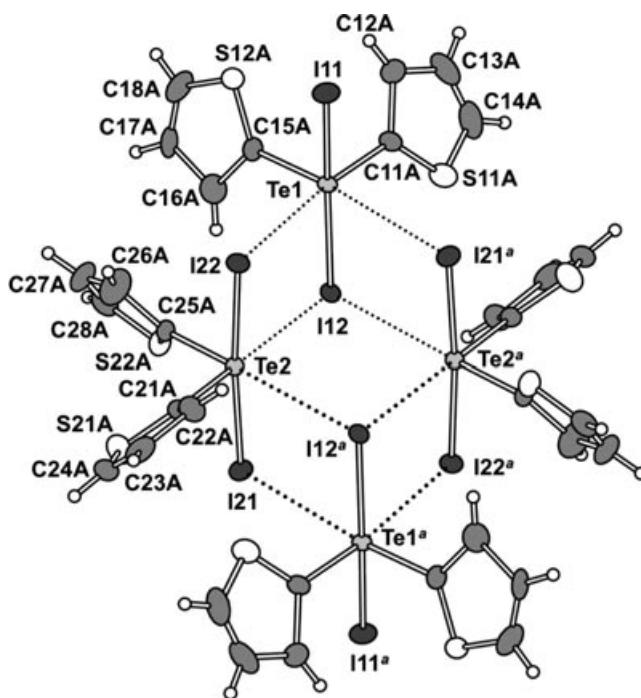


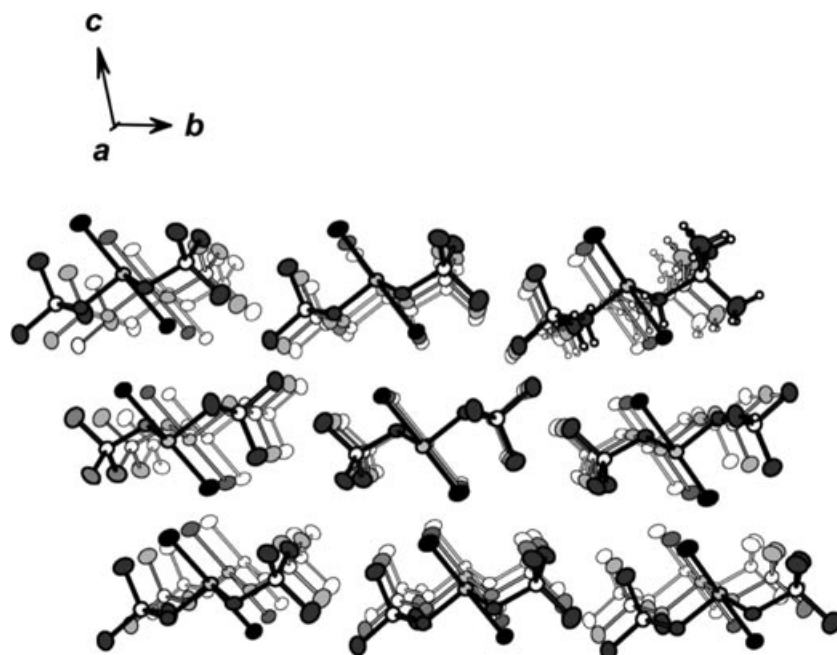
FIGURE 3 The molecular structure of Te_2Th_2 (**4**) indicating the numbering of atoms. The thermal ellipsoids have been drawn at the 50% probability level. The symmetry-equivalent tellurium and iodine atoms have been denoted by a superscript *a* (symmetry operation 1-*x*, 1-*y*, 1-*z*). The symmetry-equivalent carbon and sulfur atoms have not been denoted in the figure. Selected bond distances (Å) and angles ($^\circ$): Te1–I11 2.8407(9), Te1–I12 3.0194(10), Te2–I21 2.9319(10), Te2–I22 2.9332(10), Te1–C11A 2.118(8), Te1–C15A 2.118(8), Te2–C21A 2.110(7), Te2–C25A 2.102(8), I11–Te1–I12 171.85(2), I11–Te1–C11A 93.6(2), I11–Te1–C15A 92.6(2), I12–Te1–C11A 91.8(2), I12–Te1–C15A 93.0(2), C11A–Te1–C15A 95.1(3), I21–Te2–I22 175.71(2), I21–Te2–C21A 92.4(2), I21–Te2–C25A 90.9(2), I22–Te2–C21A 89.7(2), I22–Te2–C25A 92.6(2), C21A–Te2–C25A 95.4(3) (The bond parameters of only the most abundant orientations of the disordered thienyl rings are considered here).

for a number of related species (typical examples are shown in [3–14] and [25,26]). The molecules are packed into skewed stacks (Fig. 4) that are linked by weak I...H hydrogen bonds of 3.250(1)–3.284(1) Å.

$\text{Te}_2\text{Th}(\text{CH}_2\text{SiMe}_3)$ (**2**) and one polymorph of $\text{Te}_2\text{Ph}(\text{CH}_2\text{SiMe}_3)$ (**3a**) are isomorphous as indicated in Fig. 5. They both show relatively strong I...I interactions, but only **2** exhibits appreciable Te...I interaction (see Table 2). Furthermore, the lattices of both **2** and **3a** exhibit three-dimensional H...I hydrogen bonding network. The H...I close contacts are 3.2125(9) and 3.216(1)–3.268(1) Å for **2** and **3a**, respectively.

TABLE 2 Intermolecular $\text{Te}\cdots\text{I}$ and $\text{I}\cdots\text{I}$ Contacts (\AA) in **1–4**, Te_2Me_2 and Te_2Ph_2 That Are Shorter Than the van der Waals' Radii of the Relevant Atoms

	$\text{Te}-\text{I}$	$\text{Te}\cdots\text{I}$	$\text{I}\cdots\text{I}$	Reference
Te_2Me_2				
<i>Polymorph 1</i>				
mol 1	2.885(3)	3.919(3)	–	[25]
	2.965(3)	3.659(3)	–	[14]
mol 2	2.914(3)	3.912(3)	–	
	2.934(3)	3.826(3)	–	
mol 3	2.854(3)	3.907(3)	–	
	2.994(3)	4.030(3)	–	
<i>Polymorph 2</i>	2.9159(9)	3.7383(9)	–	
$\text{Te}_2(\text{CH}_2\text{SiMe}_3)_2$ (1)	2.8904(10)	4.229(1)	4.185(1), 4.246(1)	This work
	2.9487(10)	–	–	
$\text{Te}_2\text{Th}(\text{CH}_2\text{SiMe}_3)$ (2)	2.9098(8)	–	–	This work
	2.9512(8)	3.895(1)	3.7991(8), 4.280(1)	
$\text{Te}_2\text{Ph}(\text{CH}_2\text{SiMe}_3)$				
<i>Polymorph 1 (3a)</i>	2.9266(9)	4.108(2)	3.804(2)	
	2.9288(10)	–	3.804(2)	
<i>Polymorph 2 (3b)</i>				
mol 1	2.8992(8)	4.009(1)	4.1526(7)	
	2.9309(8)	–	–	
mol 2	2.9020(8)	–	3.7503(5)	
	2.9293(8)	3.929(1)	4.1187(7)	
Te_2Th_2 (4)				
mol 1	2.8407(9)	–	–	This work
	3.0194(10)	3.646(1), 3.660(1)	–	
mol 2	2.9319(10)	3.646(1)	–	
	2.9332(10)	3.659(1)	–	
Te_2Ph_2				
<i>Polymorph 1</i>	2.928(1)	3.955(1)	–	[26]
<i>Polymorph 2</i>				
mol 1	2.893(1)	3.926(1)	–	
	2.959(1)	–	–	
mol 2	2.883(1)	3.850(1)	–	
	2.942(1)	3.924(1)	–	

**FIGURE 4** Packing of molecules in **1**. Hydrogen atoms have been omitted for clarity.

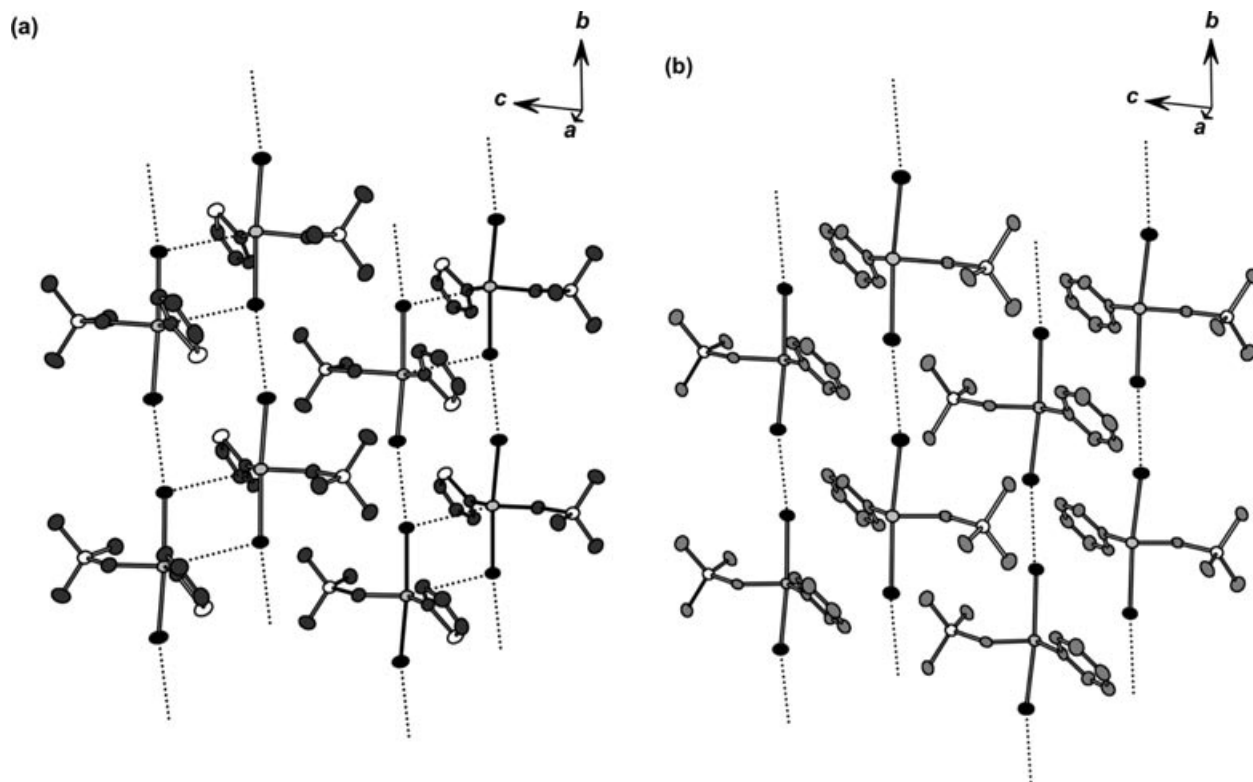


FIGURE 5 Packing of molecules in **2**. (b) Packing of molecules in **3a**. Hydrogen atoms have been omitted for clarity.

The lattice of second polymorph of TeI_2Ph (CH_2SiMe_3), **3b**, is rather interesting (Fig. 6). It is composed of two alternating layers of molecules. In one type of layer, the molecules form a continuous quasi-two-dimensional layer by both $\text{Te}\cdots\text{I}$ and $\text{I}\cdots\text{I}$ interactions (see Table 2). In the second type of layer, the molecules are linked into discrete dimers by somewhat weaker $\text{Te}\cdots\text{I}$ interactions.

The $\text{Te}\cdots\text{I}$ secondary bonds in TeI_2Th_2 (**4**) are the strongest in all molecular species considered in this work (see Table 2), and the molecules are linked into discrete tetramers, which show approximate cubic close packing in the lattice (see Fig. 7). There are no $\text{I}\cdots\text{I}$ secondary bonding interactions in **4**. Similar tetrameric $\text{Te}-\text{I}$ frameworks are also observed in $\text{TeI}_2(p\text{-C}_6\text{H}_4\text{OMe})_2$ [28] and in $\gamma\text{-TeI}_4$ [29, 30] and $\delta\text{-TeI}_4$ [31, 32]. The tetramers of **4** are linked by $\text{H}\cdots\text{I}$ hydrogen bonds of 2.9798(7)–3.3043(8) Å.

Both polymorphs in TeMe_2I_2 and TeI_2Ph_2 also show only $\text{Te}\cdots\text{I}$ interactions. These close contacts span a range of 3.659(3)–4.030(3) Å (see Table 2). The consequent supramolecular assemblies are composed of three-dimensional networks.

The influence of the secondary bonding interactions on the $\text{Te}-\text{I}$ bond lengths can clearly be seen in the data presented in Table 2. The correlation is the

clearest in the case of **4**. The iodine atom I11 shows no secondary interactions and the $\text{Te1}-\text{I11}$ is only 2.8407(9) Å. The atoms I21 and I22 are involved in one $\text{Te}\cdots\text{I}$ interaction with the $\text{Te1}-\text{I21}$ and $\text{Te1}-\text{I22}$ bond lengths of 2.9319(10) and 2.9332(10) Å, respectively. I22 shows two $\text{Te}\cdots\text{I}$ close contacts and the $\text{Te1}-\text{I12}$ is the longest tellurium–iodine bond in the molecule with the length of 3.0194(10) Å. A similar trend in the $\text{Te}-\text{I}$ bond lengths is also observed for $\text{TeI}_2(p\text{-C}_6\text{H}_4\text{OMe})_2$ [28].

The dependence of the $\text{Te}-\text{I}$ bond lengths on the $\text{Te}\cdots\text{I}$ and $\text{I}\cdots\text{I}$ interactions in the case of other molecular species listed in Table 2 is not as clear, although in a qualitative sense the same trend can be inferred. Alcock and Harrison [26] have discussed the lengthening of the $\text{Te}-\text{I}$ bond due to the secondary bonding interactions in terms of the donation of either the tellurium or iodine lone-pair to the σ^* orbital of the $\text{Te}-\text{I}$ bond. Chan and Einstein [25] have suggested that the lengthening of the $\text{Te}-\text{I}$ bond due to secondary bonding interactions increases the orbital overlap of tellurium and the iodine atom in the trans-position thereby shortening the opposite $\text{Te}-\text{I}$ bond.

The $\text{Te}-\text{C}$ bond lengths in **1–4** span a range of 2.100(6)–2.136(7) Å, and are quite close to single

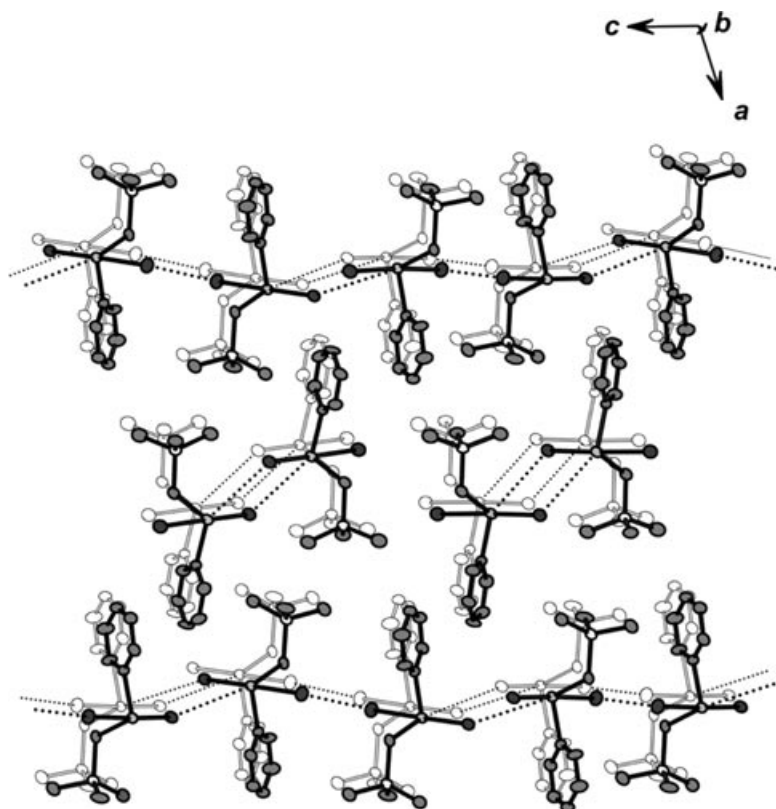


FIGURE 6 Packing of molecules in **3b**. Hydrogen atoms have been omitted for clarity.

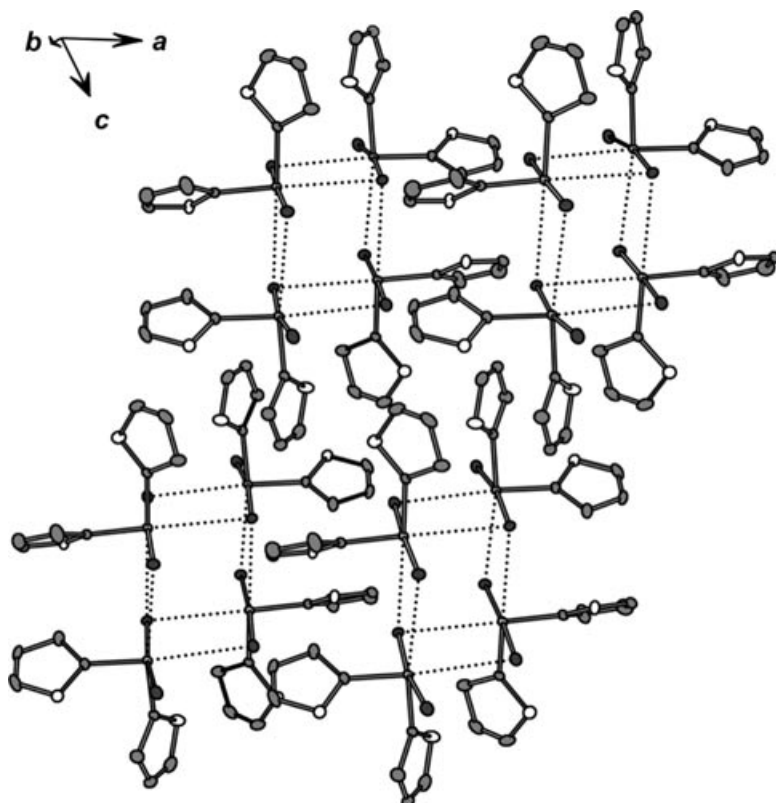


FIGURE 7 Packing of molecules in **4**. Hydrogen atoms have been omitted for clarity.

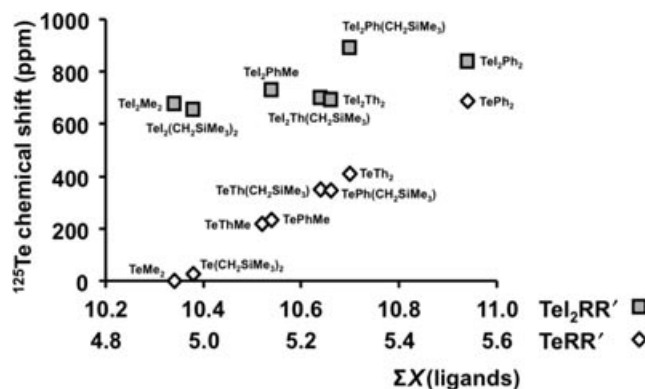


FIGURE 8 Dependence of the ^{125}Te chemical shifts of TeRR' and $\text{Te}_2\text{RR}'$ [$\text{R}, \text{R}' = \text{Me}, \text{CH}_2\text{SiMe}_3, \text{Th} (\text{C}_4\text{H}_3\text{S}), \text{Ph}$] on the electronegativities of the ligands [$\Sigma X(\text{ligands})$ denotes the sum of the electronegativities of ligands bound to tellurium].

bond lengths (the sum of the covalent radii of tellurium and carbon is 2.14 \AA [24]). They also fit well in the range of $\text{Te}-\text{C}$ bonds reported for related TeI_2R_2 molecules (as exemplified in [3–14]).

^{125}Te NMR Spectroscopy

The ^{125}Te NMR chemical shifts of compounds **1–4** as a function of the sum of the electronegativities of the ligands coordinated to tellurium are shown in Fig. 8, together with those of the corresponding tellanes. The ^{125}Te chemical shifts of TeMe_2 , TeThMe {329 ppm [33]}, TePhMe {329 ppm [34]}, TePh_2 {688 ppm [21]}, TeI_2Me_2 {675 ppm [35]}, TeI_2PhMe {698 ppm [36]}, and TeI_2Ph_2 {839 ppm [7]} are included for comparison. The electronegativities of the organic groups are estimated based on the approach by Xie et al. [37] and that of iodine is taken from the Pauling electronegativity scale [24].

It can be seen from Fig. 8 that the ^{125}Te NMR resonances of the eight tellanes exhibit a monotonic trend of shifting to higher frequencies, as the electronegativities of the organic groups bound to tellurium increase. The trend in the corresponding diiodides, however, is not as clear. Because of two relatively electronegative iodine atoms bound to tellurium, their ^{125}Te chemical shifts are expectedly found at higher resonances than those of the corresponding tellanes, but the dependence of the chemical shift on the electronegativities of the organic groups does not follow the trend as strictly. The paramagnetic contribution to the shielding at ^{125}Te nucleus plays a significant role, which is affected by the energy of the HOMO–LUMO transition [$n(\text{Te}) \rightarrow \sigma^*(\text{Te}-\text{I})$] (for the discussion of the para-

magnetic shielding in tellurium (see, for instance, [38, 39], and references therein) that is also dependent both on the nature of the organic groups bound to the $\text{Te}(\text{IV})$ center and the secondary bonding interactions involving iodine.

ACKNOWLEDGMENTS

We are grateful to P. Salin for assistance in the preparative work.

REFERENCES

- [1] Hargittai, I.; Rozsondai, B. In *The Chemistry of Organic Selenium and Tellurium Compounds*; Patai, S.; Rappoport, Z. (Eds.); Wiley: New York, 1986; Vol. 1, p. 63.
- [2] Irgolic, K. J. In *Synthetic Methods of Organometallic and Inorganic Chemistry*; Herrmann, W. A.; Cybill, C. E. (Eds.); Georg Thieme Verlag: New York, 1997; Vol. 4, p. 219.
- [3] Närhi, S. M.; Oilunkaniemi, R.; Laitinen, R. S.; Ahlgrén, M. *Inorg Chem* 2004, 43, 3742, and references therein.
- [4] Chauhan, A. K. S.; Kumar, A.; Srivastava, R. C.; Butcher, R. J. *J. Organomet Chem* 2002, 658, 169.
- [5] Asahara, M.; Taomoto, S.; Tanaka, M.; Erabi, T.; Wada, M. *Dalton Trans* 2003, 973.
- [6] Hesford, M. J.; Levason, W.; Matthews, M. L.; Orchard, S. D.; Reid, G. *Dalton Trans* 2003, 2434.
- [7] Beckmann, J.; Dakternieks, D.; Duthie, A.; Mitchell, C.; Schurmann, M. *Aust J Chem* 2005, 58, 119.
- [8] Chauhan, A. K. S.; Anamika; Kumar, A.; Srivastava, R. C.; Butcher, R. J. *J. Organomet Chem* 2005, 690, 313.
- [9] Chauhan, A. K. S.; Anamika; Kumar, A.; Srivastava, R. C.; Butcher, R. J.; Beckmann, J.; Duthie, A. *J. Organomet Chem* 2005, 690, 1350.
- [10] Block, E.; Dikarev, E. V.; Glass, R. S.; Jin, J.; Li, B.; Li, X.; Zhang, S. *Z. J. Am Chem Soc* 2006, 128, 14949.
- [11] Srivastava, P. C.; Bajpai, S.; Bajpai, S. M.; Kumar, R.; Srivastava, S.; Butcher, R. J. *Struct Chem* 2007, 18, 223.
- [12] Chauhan, A. K. S.; Singh, P.; Kumar, A.; Srivastava, R. C.; Butcher, R. J.; Duthie, A. *Organometallics* 2007, 26, 1955.
- [13] Chauhan, A. K. S.; Singh, P.; Srivastava, R. C.; Duthie, A.; Voda, A. *Dalton Trans* 2008, 4023.
- [14] Gurnani, C.; Levason, W.; Ratnani, R.; Reid, G.; Webster, M. *Dalton Trans* 2008, 6274.
- [15] Alcock, N. W. *Adv Inorg Chem Radiochem* 1972, 15, 1.
- [16] Sudha, N.; Singh, H. B.; *Coord Chem Rev* 1994, 135/136, 469.
- [17] Gysling, H. J.; Luss, H. R.; Smith, D. *Inorg Chem* 1979, 18, 2696.
- [18] Engman, L.; Cava, M. P. *Organometallics* 1982, 1, 470.
- [19] Akiba, M.; Lakshmikantham, M. V.; Jen, K. -Y.; Cava, M. P. *J. Org Chem* 1984, 49, 4819.
- [20] Ogura, F.; Otsubo, T.; Ohira, N. *Synthesis* 1983, 1006.
- [21] McFarlane, H. C. E.; McFarlane, W. *J. Chem Soc, Dalton Trans* 1973, 2416.

- [22] Altomare, G.; Cascarano, C.; Giacobozzo, A.; Guagliardi, M.; Burla, C.; Polidori, G.; Camalli, M. *J Appl Cryst* 1994, 27, 435.
- [23] Sheldrick, G. M. *Acta Crystallogr A* 2008, 64, 112.
- [24] Emsley, J. *The Elements*, 3rd ed.; Clarenton Press; Oxford, UK, 1998.
- [25] Chan, L. Y. Y.; Einstein, F. W. B. *J Chem Soc, Dalton Trans* 1972, 316.
- [26] Alcock, N. W.; Harrison, W. D. *J Chem Soc, Dalton Trans* 1984, 869.
- [27] McCullough, J. D.; Knobler, C.; Ziolo, R. F. *Inorg Chem* 1985, 24, 1814.
- [28] Farran, J.; lvarez-Larena, A. A.; Capparelli, M. V.; Piniella, J. F.; Germain, G.; Torres-Castellanos, L. *Acta Crystallogr C* 1998, 54, 995.
- [29] Beister, H. J.; Kniep, R.; Schaefer, A. *Z Kristallogr* 1986, 174, 12.
- [30] Kniep, R.; Beister, H. J.; Wald, D. *Z Naturforsch* 1988, 43, 966.
- [31] Krebs, B.; Paulat, V. *Acta Crystallogr B* 1976, 32, 1470.
- [32] Paulat, V.; Krebs, B. *Angew Chem* 1976, 88, 28.
- [33] Oilunkaniemi, R.; Komulainen, J.; Laitinen, R. S.; Ahlgrén, M.; Pursiainen, J. *J Organomet Chem* 1998, 571, 129.
- [34] O'Brien, D. H.; Dereu, N.; Huang, C. -K.; Irgolic, K. J.; Knapp, F. F. *Organometallics* 1983, 2, 305.
- [35] Chadha, R. K.; Miller, J. M. *Can J Chem* 1982, 60, 596.
- [36] McFarlane, W.; Berry, F. J.; Smith, B. C. *J Organomet Chem* 1976, 113, 139.
- [37] Xie, Q.; Sun, H.; Xie, G.; Zhou, J. *J Chem Inf Comput Sci* 1995, 35, 106.
- [38] Luthra, N. P.; Odom, J. D. In *The chemistry of organic selenium and tellurium compounds*; Patai, S.; Rappoport, Z. (Eds.); Wiley: New York 1986; Vol. 1, p. 229.
- [39] Fleischer, H.; Mitzel, N. W.; Schollmeyer, D. *Eur J Inorg Chem* 2003, 815.